

2008

A-Type Heat Exchanger Simulation Using 2-D CFD for Airside Heat Transfer and Pressure Drop

Omar Abdelaziz
University of Maryland

Varun Singh
University of Maryland

Vikrant Aute
University of Maryland

Reinhard Radermacher
University of Maryland

Follow this and additional works at: <http://docs.lib.purdue.edu/iracc>

Abdelaziz, Omar; Singh, Varun; Aute, Vikrant; and Radermacher, Reinhard, "A-Type Heat Exchanger Simulation Using 2-D CFD for Airside Heat Transfer and Pressure Drop" (2008). *International Refrigeration and Air Conditioning Conference*. Paper 865.
<http://docs.lib.purdue.edu/iracc/865>

This document has been made available through Purdue e-Pubs, a service of the Purdue University Libraries. Please contact epubs@purdue.edu for additional information.

Complete proceedings may be acquired in print and on CD-ROM directly from the Ray W. Herrick Laboratories at <https://engineering.purdue.edu/Herrick/Events/orderlit.html>

A-Type Heat Exchanger Simulation Using 2-D CFD for Airside Heat Transfer and Pressure Drop

Omar AbdelAziz^{1*}, Varun Singh², Vikrant Aute³, Reinhard Radermacher⁴

Center for Environmental Energy Engineering
Department of Mechanical Engineering, University of Maryland
College Park, MD 20742 USA

¹Tel: 301-405-8726, Fax: 301-405-2025, Email: oabdelaz@umd.edu

²Tel: 301-405-8726, Email: vsingh3@umd.edu

³Tel: 301-405-8726, Email: vikrant@umd.edu

⁴Tel: 301-405-5286, Email: raderm@umd.edu

* Corresponding Author

ABSTRACT

A-Type heat exchangers are used to meet required heat load with minimum duct dimensions in air-conditioning applications. This greatly reduces the air-conditioning system footprint in residential and commercial applications. The angle and tube spacing of the A-type heat exchangers should be optimized for minimum duct size and maximum heat load. However, existing air side heat transfer and pressure drop correlations may not be applicable for A-type heat exchangers due to non-uniform air velocity profile and temperature distribution in the heat exchanger. In this paper, a new technique is proposed where a segment-by-segment $\varepsilon - NTU$ based coil model is coupled with automated 2-D CFD simulations of air flow through the heat exchanger. The 2-D CFD simulations are used to calculate the heat transfer coefficient on each tube as well as the inlet air velocity profile on the coil face. The segmented $\varepsilon - NTU$ solver calculates NTU based on the CFD calculated heat transfer coefficient on the airside, the refrigerant side heat transfer (from available correlations), and tube-fin arrangement. In the current investigations, a parametric study was performed by varying the tube pitch, row pitch and the coil angle. The proposed framework is used to automatically generate the mesh and run the 2-D double precision CFD simulations using commercial CFD tools for the different configurations. The $\varepsilon - NTU$ calculations are performed using a validated segment by segment fin and tube heat exchanger model developed by the authors. The simulation results for each coil configuration were compared against the base line heat exchanger configurations. The trade-off between the heat exchanger enclosure volume and material cost is presented.

1. INTRODUCTION

Refrigerant to air fin-and-tube heat exchangers are widely used in the refrigeration and air conditioning industry to transfer heat between air and working fluid (e.g., refrigerant, water, glycols etc.) In order to predict their performance accurately and reduce design & development time, computer models are fast replacing physical prototypes. There are several such models and tools in the literature used to model both steady state and transient behavior that have been validated against experimental results. (Singh et al., 2008, Jiang et al., 2006, Liu et al., 2004, Oliet et al., 2002, Liang et al., 2001, Domanski, 1999)

Most residential air conditioning applications employ an A-type heat exchanger (A-coil) for indoor conditioning. This coil serves as an evaporator in air conditioning mode and a condenser in heat pumping mode. Most heat exchanger models employ an air velocity/flow profile at the coil face, and assume it is propagated through the coil, perpendicular to tube banks. In this regard, simulation of A-coils presents a unique challenge because air inlet through the duct is not perpendicular to the coil face. However, Chwalowski et al. (1989) conducted air visualization experiments for various coil slab configurations and angles, and found that the air velocity is predominantly perpendicular to the coil face. This key result has been widely used as a fundamental assumption in several validated

heat exchanger simulations (Domanski, 1991, Wang, 2008). Recently, Domanski and Yashar (2007) used Particle Image Velocimetry to obtain the air velocity profile through an A-coil, and used these measurements to validate their Computational Fluid Dynamics (CFD) simulation results for an A-coil. These results showed air flow maldistribution inside the coil. When dealing with such maldistribution, optimization of a heat exchanger assumes critical importance.

Heat exchanger optimization has been an area of significant work for the air conditioning and refrigeration community, for over four decades. A heat exchanger optimization problems has both continuous (tube length etc.) as well as discrete (off-the-shelf tube diameters etc.) variables. With the advent of evolutionary algorithms (Holland 1975, Goldberg 1989, Deb 2001), and their capability of handling discrete as well as continuous variables of an optimization problem, heat exchanger optimization has become an area of active research. Aute *et al.* (2004) used a multiobjective genetic algorithm (MOGA) to optimize a condenser for maximum heat load and minimum cost, and obtained a set of Pareto optimal solutions. Domanski and Yashar (2007) used symbolic learning based optimization algorithm to optimize the circuitry of a condenser coil.

2. MULTI-LEVEL HYBRID SIMULATION APPROACH

The evaluation of A-coil performance requires the knowledge of the inlet air profile. This profile is a function of the coil inclination as well as tube vertical and horizontal spacing. Furthermore, the airflow propagation through the coil is not normal to the face area as in conventional heat exchanger designs, which means that the airside heat transfer coefficient correlations for airflow across a tube bank might not be valid. Nevertheless, the inclination of the coil and the top plate position, as shown in Figure 2a below, could lead to a recirculation region that penalizes some of the top tubes' performance for a down flow configuration. In this research a new multi-level hybrid simulation approach is introduced where the airside velocity distribution and heat transfer coefficients are calculated based on CFD simulations. Furthermore, this simulation approach is integrated with a MOGA routine for cost and volume optimization. The flow chart of this multi-level simulation approach is shown in Figure 1 below. The entire approach is packaged into a single framework that does not need manual intervention. In this case, mesh generation, CFD simulations and post processing are automated. The following sections provide a brief description of each of the simulation approach components.

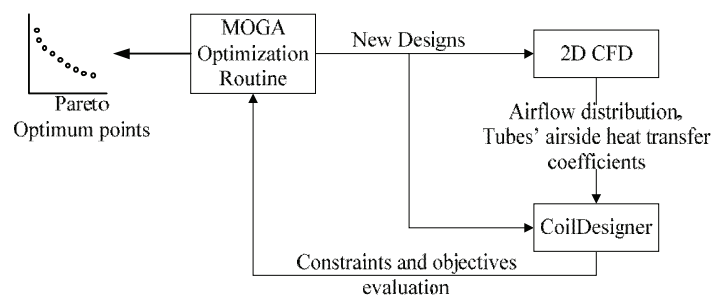


Figure 1: Optimization using multi-level simulation

2.1 MOGA Optimization Routine

The MOGA optimization routine is used to generate a population of design points. For each candidate design in the population, the objectives and constraints are evaluated using the integrated multi-level simulation tool. Based on the objectives' values and the constraints' violations, the MOGA routine ranks the population and creates a new subset of design points for replacement through genetic operations. The non-dominated points are carried over from one generation to the next. The optimization routine is allowed to run for a specific number of generations. The reader is referred to Deb (2001) for more details.

2.2 CFD simulations

The CFD simulations are performed using a commercially available CFD package. Instead of simulating the whole heat exchanger, the simulation domain is reduced by considering appropriate periodicity and symmetry planes. This helps in offsetting the computational effort and reduces the evaluation time. For a finned tube heat exchanger, the domain can be simplified to simulate the flow between 2 fins or even a 2-D flow can be assumed. Navier-Stokes and energy equations are solved along with an appropriate turbulence closure model using Fluent® (Kim *et al.*, 1998).

Initial studies on mesh independence and turbulence model validity and further model tuning were performed before solver integration.

2.3 ϵ -NTU Based Solver

The heat exchanger model developed by Jiang *et al.* was employed. This model divides the heat exchanger into several tube-fin macro volumes, and employs the effectiveness-NTU (ϵ -NTU) method to solve for outlet states of the two fluids. To allow generalized circuitry, the model employs a junction-tube connectivity matrix which is used to track refrigerant flow from inlet to outlet of the heat exchanger. The computational sequence is generated at run-time based on heat exchanger circuitry. The model distributes mass flow rate through circuits of different length, based on pressure drop. In the current work, the circuits were made of equal length and hence refrigerant mass flow was evenly distributed among circuits. Furthermore, the heat exchanger is discretized into tube-fin macro volumes to account for non-uniform distribution of air flow on coil face, as well as accurate calculation of heat load and pressure drop through the tubes.

3. PROBLEM DESCRIPTION

The hybrid simulation approach discussed in Section 2 is used to simulate the performance of a 10 kW A-coil R410A condenser. Two dimensional CFD simulations are used to evaluate the inlet air velocity profile to the heat exchanger as well as the heat transfer coefficient for each tube. The airside pressure drop from the 2-D CFD simulations is underestimated due to the absence of fin wall friction; hence, the pressure drop is evaluated based on the average face velocity magnitude and conventional pressure drop correlations (Kim *et al.* (1999)). Further, the heat exchanger cost was calculated assuming material costs associated with copper (for tubes) and aluminum (for fins). Copper price was assumed to be \$6.00/kg and aluminum was assumed to be \$4.00/kg. Figure 2 below illustrates the A-coil considered in the current work where air is flowing from top to bottom. The CFD simulations are performed for an x-y plane at the mid point of the tube length as shown in Figure 2a. Further reduction to the computational domain can be achieved by the identified symmetry plane. The simplified computational domain considered in the present work is illustrated in Figure 2b. During optimization the following coil parameters were fixed: coil circuitry, tube inner and outer diameters, fin type and thickness, inlet air state and flow rate and refrigerant inlet state and mass flow rate. The values of these parameters are summarized in Table 1 below with the coil circuitry shown in Figure 2a.

Table 1: Optimization Parameters

Parameter	Value	Unit	Parameter	Value	Unit
Inner diameter	0.0094	M	inlet air flow rate	0.284	m ³ /s
Outer diameter	0.0105	M	inlet air temperature	294.15	K
Tube banks per side	3	(-)	inlet air relative humidity	43.46	%
Number of tubes per bank	18	(-)	inlet refrigerant flow rate	0.0212	kg/s
Fin thickness	0.1	mm	inlet refrigerant pressure	2.6525	MPa
Fin type	Louver	(-)	inlet refrigerant temperature	345.55	K

3.1 Optimization Problem

The baseline A-coil is a conventional A-coil used in commercial 10 kW air conditioning systems (Wang (2008)). The objectives of the coil optimizations are to minimize the material cost as well as minimizing the enclosure volume. The first objective would reflect potential savings in final product costs while the second objective reflects the savings in the real-estate footprint of the air conditioning equipment in a typical residential application.

Airside pressure drop, heat load and volume constraints are imposed on the optimization problem in order to identify acceptable heat exchanger designs. The air pressure drop is constrained to be less than 100 Pa (baseline pressure drop is 81 Pa). In order to find heat exchangers with smaller enclosure volume than the baseline system (baseline volume = 0.095322 m³), designs with larger enclosure volumes are considered infeasible. Finally, all prospective heat exchanger designs must provide the same heat load as the baseline system, hence only a $\pm 5\%$ difference from the baseline heat load was allowed (baseline heat load = 10873.606 W).

The optimization variables included in this study are: tube length, slab inclination angle, number of fins per inch, tube horizontal spacing and tube vertical spacing. These variables are defined as continuous variables in the MOGA routine with a bit-length of 4 (16 values) for each variable. Baseline values, range and precision of these variables

are shown in Table 2. The MOGA population size was set to 100 with a replacement of 10%, and it was set to run for 200 iterations. This resulted in a total of 2200 function evaluations out of a possible 1048576 (16^5).

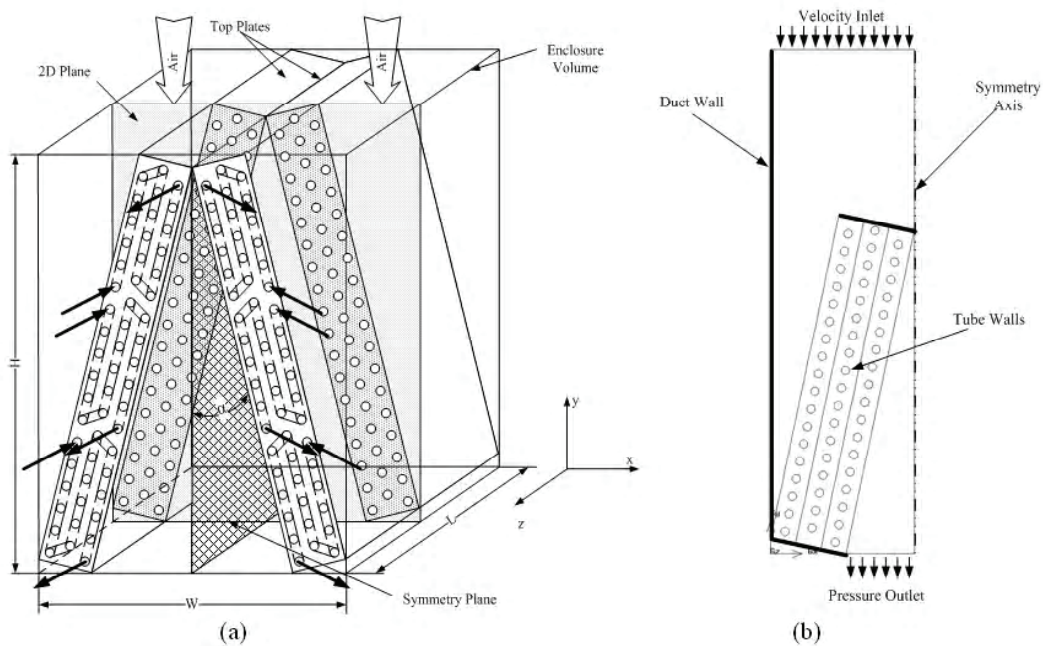


Figure 2: A-coil configuration

Table 2: Optimization variables

Variable	Baseline value	Range	Precision	Unit
Tube Length	0.46	0.3174 - 0.736	0.028	m
Inclination angle (α)	18.5	10 - 40	2	$^{\circ}$
FPI	14	9 - 24	1	(-)
HS	0.0205	0.0173 - 0.0346	0.00116	m
VS	0.0265	0.0159 - 0.0448	0.00193	m

3.2 Geometry and Mesh Generation

A code was developed to generate Gambit® journal file based on the variables' values populated by the MOGA optimizer. The computational domain was based on the values of α , HS and VS. Triangular pave mesh is used everywhere with different mesh sizes as shown in Figure 3. For improved resolution of the flow field, quadrilateral inflated mesh is used to discretize the domain in the vicinity of tubes. In addition, inflated mesh is used near the wall boundaries for a better resolution of the boundary layer. As described in Figure 2b, air inlet is set as a velocity inlet boundary condition, air outlet is set as pressure outlet, and the centerline is set as a symmetry boundary condition.

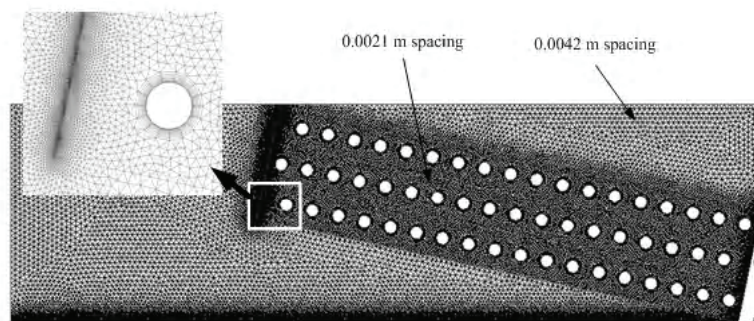


Figure 3: Automated mesh generation

3.3 CFD Simulations and Post Processing

Another code was integrated in the framework to generate journal files for the Fluent® runs based on the variables for each design. The inlet velocity for each case is calculated as shown in equation (1) below taking into account the new coil dimensions. The inlet air temperature was kept constant for all cases at 294.15 K. Tubes' wall temperatures were set to the saturation temperature (317.15 K) based on the inlet refrigerant pressure. Based on preliminary investigations of the turbulence models for this problem, RNG k- ϵ model provided the highest stability and best convergence. Therefore, it was used for the turbulent closure equations. The built in two-layer model with enhanced wall treatment was enabled including the pressure gradient and thermal effects in the boundary layer for improved solution of the viscosity affected region. The Green-Gauss Node-Based gradient evaluation was used for a better representation of the unstructured mesh solution. Second order discretization scheme was used for pressure, momentum and energy equations while a first order upwind scheme was used for the k and ϵ equations. The air properties are evaluated based on ASHRAE fundamentals (2005). The solver was allowed to iterate up to 1000 iterations or until a convergence was achieved. Convergence criteria were based on minimum acceptable residuals of 10^{-3} for all equations except the energy equation which was set to 10^{-6} .

After the solution converges, inlet air velocity for the first tube bank, and upstream temperature and total surface heat flux for each tube were written to a file for further post processing. These data were used to update the ϵ -NTU solver's coil face velocity and tubes' airside heat transfer coefficients. The airside heat transfer coefficient is calculated based on the tube total heat flux, wall temperature and incoming air temperature as shown in equation (2).

$$V = \frac{0.284}{L \times 2 \times (18.5 \times VS \times \sin(\alpha) + 3 \times HS \times \cos(\alpha))} \quad (1)$$

$$h_{air} = \frac{q''}{(T_{wall} - T_{air,in})} \quad (2)$$

4. OPTIMIZATION RESULTS

After 200 MOGA optimization iterations, 136 distinct feasible designs were identified. The Pareto optimal set was found to include 7 designs as shown in Figure 4. The feasible domain is bounded by heat exchanger designs having material costs between \$44 and \$21.9 with enclosure volume ranging from 0.0647 to 0.0953 m^3 . The Pareto optimal designs are summarized in Table 3. It is interesting to note that the slab inclination angle of all Pareto optimal solutions was less than the baseline coil. Fins per inch are seen to be high for coils with higher volumes and angles, and low for coils with low volume and smaller angles. This is dictated by the air pressure drop constraint. Higher fin density leads to higher pressure drop, but air velocity is reduced when the angle, and accompanying volume, is large. However, with lower angles and coil volumes, the fins per inch are lower to mitigate the pressure drop effects of higher velocity.

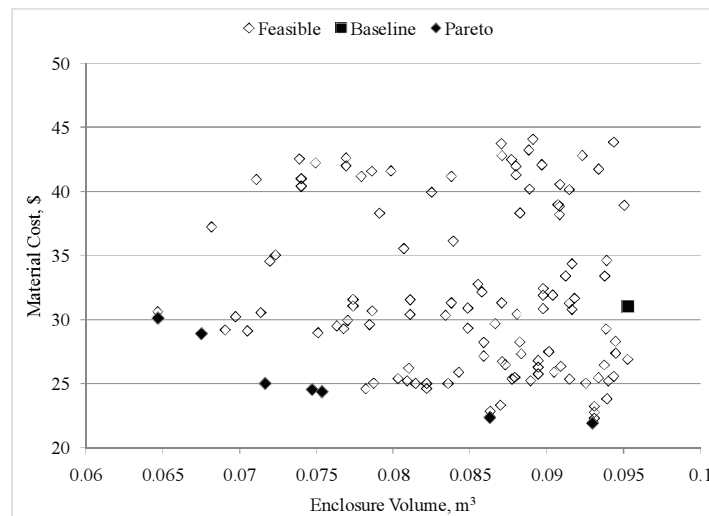


Figure 4: Feasible designs cost versus enclosure volume

Table 3: Pareto optimum set designs

Coil No.	α , °	HS, mm	VS, mm	L, mm	FPI	V_3 , m ³	C, \$	ΔP_{air} , Pa	Q, W	h_{air} , W/m ² K	ΔP_{ref} , Pa	V savings, %	C savings, %
BL	18.5	20.5	26.5	460	14	0.0953	30.8	81.3	10874	44.4	2936.6	0	0
1	10	17	26	513	9	0.0647	30.1	87.0	10738	53.3	3307.4	32.1	2.9
2	14	18	24	485	10	0.0675	28.9	89.7	10358	50.8	3306.9	29.2	6.8
3	14	18	27	401	11	0.0717	25.0	85.3	10341	52.3	2756.3	24.8	19.3
4	14	18	29	373	13	0.0747	24.5	98.7	10508	52.5	2453.0	21.6	20.8
5	16	21	27	373	12	0.0754	24.4	98.1	10370	51.6	2541.3	20.9	21.4
6	14	18	35	317	14	0.0863	22.3	86.4	10503	52.2	2158.0	9.4	27.9
7	16	17	35	317	14	0.0930	21.9	66.7	10360	48.6	2350.2	2.4	29.2

To further understand the results, two coils which bound the Pareto optimal points, lowest cost and highest volume – coil 7, and highest cost and lowest volume – coil 1, were studied further. Figure 5 shows the air velocity vectors for coil 7. Due to flow stagnation near the top of the coil, a recirculation zone can be seen inside the coil. For the current case, this recirculation zone encompasses 14 tubes. The air velocity vectors show that the coil behaves more like an inline coil with respect to air flow. This also leads to the lowest air side pressure drop in this coil. Such a flow pattern also leads to a higher number of fins per inch to achieve the desired heat load. Figure 6 shows velocity vectors for coil 1. It is seen that the number of tubes in the recirculation wake of the air flow is nearly the same as that for coil 7. However, the tube length is high but this is compensated by small vertical spacing. Further, due to higher velocity associated with smaller volume, the fins per inch are the least of all cases to avoid any potential violation of the air side pressure drop constraint. Observing the air velocity vectors, it is interesting to note that the coil behaves more like a staggered coil, when compared to coil 7.

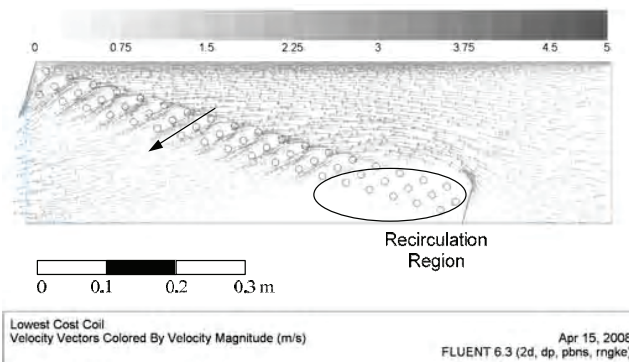


Figure 5: Lowest cost coil velocity vectors

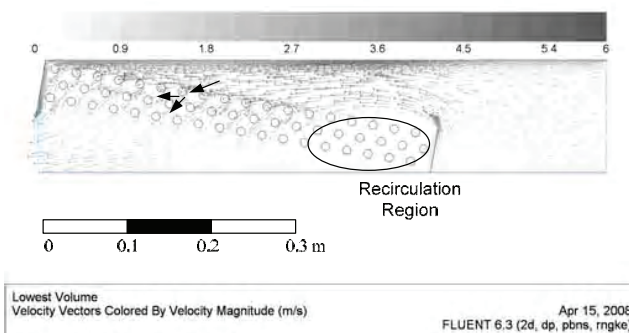


Figure 6: Lowest volume coil velocity vectors

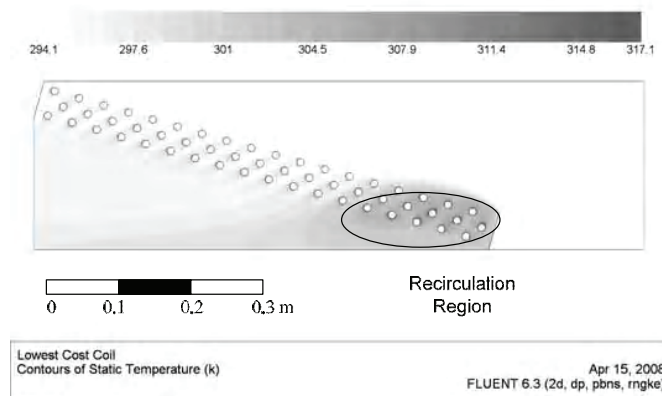


Figure 7: Lowest cost coil temperature profiles

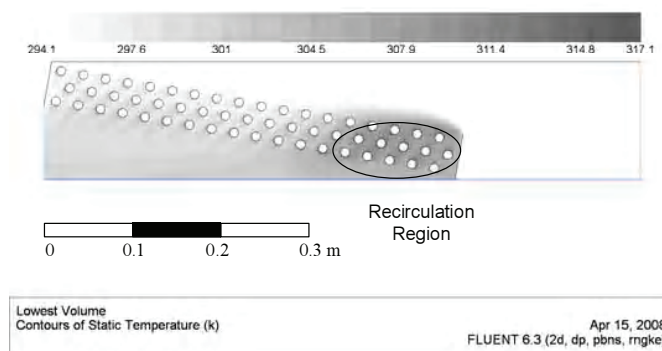


Figure 8: Lowest volume coil temperature profiles

The temperature profiles for the A-coils 1 and 7 are shown in Figures 7 and 8. The recirculation zone can be easily identified by the higher air temperature. The low air flow velocity along with the high air temperature reduced the total tube heat flux for the tubes in the recirculation region and penalized the A-coil performance. For the smallest volume design, the average total tube wall heat flux was 1026.2 W/m^2 with the minimum being 140 W/m^2 for tubes in the recirculation region and the maximum being 1922.7 W/m^2 for tubes closer to the bottom in the first bank. This resulted in an average airside heat transfer coefficient of $53 \text{ W/m}^2\text{K}$ with a standard deviation of $21 \text{ W/m}^2\text{K}$ between the tubes.

5. CONCLUSIONS

A new concept of multi-level heat exchanger simulation was proposed and developed. Initial investigations showed that the model can be used in optimization due to the lower computational cost compared to full scale CFD simulations of heat exchangers. This approach was used along with MOGA to minimize the A-coil enclosure volume and material cost. The use of MOGA reduced the number of function evaluations from 16^5 , for exhaustive search, to only 2200. The Pareto optimal set contained 7 designs. These designs showed a trade-off in enclosure volume reduction and material cost ranging from a 32.1 % reduction in enclosure volume at 2.9% reduction in cost to a 2.4% reduction in volume at 29.2% cost reduction. For the smallest volume design, the heat exchanger tubes showed a pseudo staggered tube bank configuration with respect to bulk air flow direction whereas for the least cost design with minimum airside pressure drop, the configuration behaved like an inline tube bank. Future work direction should include the study of individual coil circuits in addition to the entire heat exchanger. The ϵ -NTU solver assumed a normal velocity propagation which might not hold true for all configurations. A segmented heat exchanger model with adaptive airside propagation would increase the accuracy of simulation. In addition to the existing variables, other variables (coil circuitry, air flow direction, fixing plate design, etc.) can be included in future studies.

NOMENCLATURE

C	material cost	(\$)	V	Volume	m ³
FPI	fins per inch	(-)	VS	Vertical Spacing	m
<i>h</i>	heat transfer coefficient	(W/m ² K)	α	bank inclination angle	(°)
HS	tube horizontal spacing	(m)	ΔP	pressure drop	(Pa)
<i>k</i>	turbulence kinetic energy	(m ² /s ³)	ε	effectiveness	(-)
L	tube length	(m)	ε	turbulence dissipation rate	(m ² /s ³)
NTU	Number of Transfer Units	(-)	Subscripts		
Q	heat load	(W)	ref	refrigerant	
RNG	renormalization groups	(-)			

REFERENCES

- ASHRAE, 2005, *ASHRAE Handbook of fundamentals (SI Edition)*, ASHRAE, GA, USA p.
- Aute, V.A., Radermacher, R., Naduvath, M.A., 2004, Constrained Multi-Objective Optimization of a Condenser Coil Using Evolutionary Algorithms, *10th Int. Ref. and A-C Conf. at Purdue*
- Chwalowski, M., Didion, D. A., Domanski P.A., 1989, Verification of Evaporator Models and Analysis of Performance of an Evaporator Model, *ASHRAE Trans.*, vol. 95, part 1.
- Deb, K., 2001, *Multi-Objective Optimization Using Evolutionary Algorithms*, Wiley and Sons.
- Domanski, P. A., 1991, Simulation of an Evaporator with Non-uniform One Dimensional Air Distribution, *ASHRAE Trans. Symposia*, NY-91-13-1.
- Domanski, P.A., 1999, Finned-Tube Evaporator Model with a Visual Interface, *Int. Congress of Refrig.*
- Domanski, P.A., Yashar, D., 2007, Application of an Evolution Program for Refrigerant Circuitry Optimization, *Challenges to Sustainability. ACRECONF Proc.*, p. 1-16.
- Finite-Volume Scheme, 36th Aerospace Sciences Meeting & Exhibit, January 12-15, 1998 / Reno, NV, p.1-11 AIAA 98-0231
- Goldberg, D.E., 1989, *Genetic Algorithms in Search, Optimization and Machine Learning*, Addison-Wesley
- Holland, J.H., 1975, *Adaption in Natural and Artificial Systems*, University of Michigan Press.
- Jiang, H., Aute, V., Radermacher, R., 2006, CoilDesigner: A General-purpose Simulation and Design Tool for Air-to-Refrigerant Heat Exchangers, *Int. J. Refrig.*, vol. 29, p. 601-610.
- Kim, N.H., Yun, J.H., Webb, R.L., 1999, Heat Transfer and Friction Correlations for Wavy Plate Fin-and-Tube Heat Exchangers, *ASME Trans.*, vol. 119, p. 560-567
- Kim, S.E., Mathur, S.R., Murthy, J.Y., Choudhury, D., 1998, A Reynolds-Averaged Navier-Stokes Solver Using
- Liang, S.Y., Wong, T.N., Nathan, G.K., 2001, Numerical and Experimental Studies of Refrigerant Circuitry of Evaporator Coils, *Int. J. Refrig.*, vol. 24, p. 823-833.
- Liu, J., Wei, W., Ding, G., Zhang, C., Fukaya, M., Wang, K., Inagaki, T., 2004, A General Steady State Mathematical Model for Fin-and-Tube Heat Exchanger based on Graph Theory, *Int. J. Refrig.*, vol. 27, p. 965-973
- Oliet, C., Perez-Segarra, C.D., Danov, S., Oliva, A., 2002, Numerical Simulation of Dehumidifying Fin-and-Tube Heat Exchangers: Modeling Strategies and Experimental Comparisons, p. 1-8.
- Singh, V., Aute, V., Radermacher, R., 2008, Numerical Approach for Modeling of Air-to-Refrigerant Fin-and-Tube Heat Exchanger with Tube-to-Tube Heat Transfer, *Int. J. Refrig.*, DOI 10.1016/j.ijrefrig.2008.03.013
- Wang, X., 2008, Performance Investigation of Two Stage Heat Pump System with Vapor Injected Scroll Compressor, *Doctoral Thesis, University of Maryland, College Park, MD.*